Combinatorial study of MZO emitters for CdTe-based solar cells

Yegor Samoilenko,[1] Gavin Yeung,[1] Andriy Zakutayev,[2] Matthew O. Reese,[2] and Colin A. Wolden[1]

[1] Colorado School of Mines, Golden, CO 80401, USA

[2]National Renewable Energy Laboratory, Golden, CO 80401, USA

***Abstract* — Precise band alignment at the front interface of CdTe-based solar cells is necessary to reduce photoexcited charge carrier recombination and to enable higher energy conversion efficiencies. Magnesium zinc oxide is not only transparent but also offers the ability to tune the conduction band offset with CdTe at the front of the device stack. In this work, we describe reactive sputtering of $Mg_{1-x}Zn_xO$ using metal targets and its application in CdTe photovoltaics. Combinatorial libraries of $Mg_{1-x}Zn_xO$ were created to tune the conduction band alignment for the optimal performance of CdTe solar cells. Band gap variation of more than 0.4 eV is achieved across a 3-inch substrate. Kelvin probe measurements demonstrate variance of work function across the substrate. Device performance is optimized at band gaps of 3.5 eV for the CdTe device processing conditions employed in this study.**

***Index Terms* — buffer layer, cadmium telluride, band alignment, Kelvin probe, magnesium zinc oxide.**

I. Introduction

Cadmium telluride (CdTe) is the leading commercialized thin-film photovoltaic (PV) technology with record device efficiency currently at 22.1% [1]. Although short circuit current density (J_{sc}) values have been improved by incorporation of Se and elimination of CdS as a window layer [2], open circuit voltage (V_{oc}) is still well below its theoretical maximum. The road towards high V_{oc} and 25% devices requires a combination of low interface recombination velocity, higher lifetime, and higher carrier concentration in the CdTe absorber [3].

$Mg_{1-x}Zn_xO$ (MZO) has been successfully used by several groups as an alternative to CdS [4, 5], which absorbs a significant amount of light due to its band gap of 2.4 eV. MZO offers tunability of the band gap above 3.3 eV which allows more light to reach the CdTe absorber. Recent findings also suggested that MZO might play a role in passivating the front interface [6]. The conduction band alignment of MZO with CdTe can be adjusted for optimal performance by varying Mg content. Flat or slightly positive conduction band offset has been suggested to produce optimal performance [3, 4, 5, 7].

It was previously reported that MZO with a band gap of around 3.7 eV produces optimal performance in a CdTe device due to formation of a favorable conduction band alignment at the front of the device [2, 4]. However, it was also reported recently that properties of MZO may change depending on subsequent processing conditions, namely CdTe deposition and $CdCl_2$ treatment [5]. Specifically, Mg content drop was observed in a film that was pre-heated prior to CdTe deposition, as well as that from a "peeled" device. To date most efforts have employed ceramic MZO targets [4, 5, 8, 9] which limits one to discrete compositions, results in slower deposition rates, and is expensive.

The goals of this work are two-fold. First, we demonstrate successful synthesis of MZO films through reactive co-sputtering using metal targets. Uniform films are deposited with substrate rotation while combinatorial libraries are created with the substrate fixed to fine-tune the optimal MZO composition for CdTe-based solar cells. The use of combinatorial libraries allows us to probe multiple compositions, and therefore, band gaps of MZO, on a single substrate, reducing the effect of processing variability [10]. Importantly, since Mg content has been noted to change with CdTe growth temperatures, this enables CdTe and $CdCl_2$ conditions to be optimized independent of the MZO composition. Hence, optimal MZO parameters for a low temperature deposition CdTe process might be different than those for a high temperature process, but both can quickly be identified.

II. Materials and Methods

MZO films were deposited in a combinatorial fashion by co-sputtering in an AJA Orion-5 chamber. TEC10 glass (Hartford Glass) superstrates were used for devices and glass slides and Si wafers for band gap and thickness measurements, respectively. Process windows were identified that resulted in both ZnO and MgO films of high quality from metal (99.99% and 99.95%, respectively) targets at appropriate rates. Argon and oxygen were supplied in a 2:1 ratio at P = 5 mTorr, which enabled significant rates while ensuring that the deposited films were fully oxidized. DC and RF sputtering was used for Zn and Mg targets, respectively. Upon calibration of the deposition rate of the individual oxides, libraries with thickness variation in the range of 80 to 200 nm across a 3-inch substrate were deposited at rates of 1.2-3 nm/min. UV-Vis and ellipsometry were used to determine band gap and thickness of MZO, respectively. Work function measurements were performed on MZO thin films using Kelvin probe. For devices, MZO was deposited on commercially available TEC10 glass (Hartford Glass) that was cleaned with Micro 90 solution and UV-ozone for 20 min. In addition, substrates were plasma-cleaned at 50W for 5 min in pure Ar at 5 mTorr prior to MZO depositon. CdTe absorbers 4 μm in thickness were deposited on top of SnO_2:F (FTO)/MZO superstrates using vapor transport deposition at 420ºC. N_2 was

used as a carrier gas at 375 sccm, while O_2 was supplied in the background at 10% of the N_2 flow rate. After CdTe deposition, samples underwent a $CdCl_2$ treatment at 430ºC for 30 min in a 50/50 vol% O_2/N_2 atmosphere. Samples were then etched in bromine/methanol mixture to form a Te-rich layer prior to ZnTe:Cu co-evaporation at 100ºC. Alternatively, some devices were made without ZnTe:Cu layer. In that case, $CdCl_2$-treated samples were rinsed in DI water for 10 s, soaked in 0.1 mM solution of $CuCl_2$ for 2 min, rinsed with DI water for 30 s and annealed on the hotplate for 30 min at 170-180 ºC. Finally, Au was evaporated through a patterned mask to create a back contact. Devices (0.079 cm^2) were isolated by manual scribing and indium was soldered on top of TCO to create a front contact. For devices employing ZnTe:Cu layer, activation of the back contact was done using rapid thermal annealing at temperatures of 280-300 ºC for 30 seconds. Current density-voltage (J-V) curves were generated in a Solar Simulator for each device under 1-sun illumination.

III. Results and Discussion

A. ZnO and MgO sputtering

Prior to depositing MZO films, both Zn and Mg were sputtered separately in Ar:O_2 ambient to determine the optimal conditions and rates for ZnO and MgO. DC sputtering was examined first, as it is more cost effective. DC sputtering of Zn in a 2:1 Ar:O_2 was studied in current controlled mode at ambient temperature. The plasma was stable over a wide range and the deposition rate was proportional to the current density. A critical current density of 7 mA/cm^2 was identified. Films deposited below this threshold were phase pure and stress-free as measured by XRD, transparent, and too insulating to be measured by four point probe. Above this threshold one observed indications of unoxidized zinc incorporation in the films.

In contrast to ZnO, the operating window for DC reactive sputtering of high quality MgO was quite limited due to a very abrupt transition between metallic mode and oxide mode. The rates were very high in the former and very low in the latter, and neither were compatible with what was required to form MZO alloys with the desired compositions. However it was found that RF sputtering resulted in stable operation across a wide range of conditions and the resulting films were XRD amorphous, transparent, and highly insulating. The deposition rate scaled linearly with RF power density over a wide range (2 – 10 W/cm^2), which enabled fabrication of MZO alloys with appropriate composition.

Figure 1 shows the placement of the targets used for combinatorial sputtering along the plane as well as the spatial variation in deposition rates of the individual oxides along the line between the two targets. The rates variation between the two targets was +/-50% of the rate obtained under rotation (horizontal lines). It is interesting that the relative variation in the MgO deposition rate was less than ZnO, and this was attributed to the visibly different shapes of the plasma plumes emanating from each target.

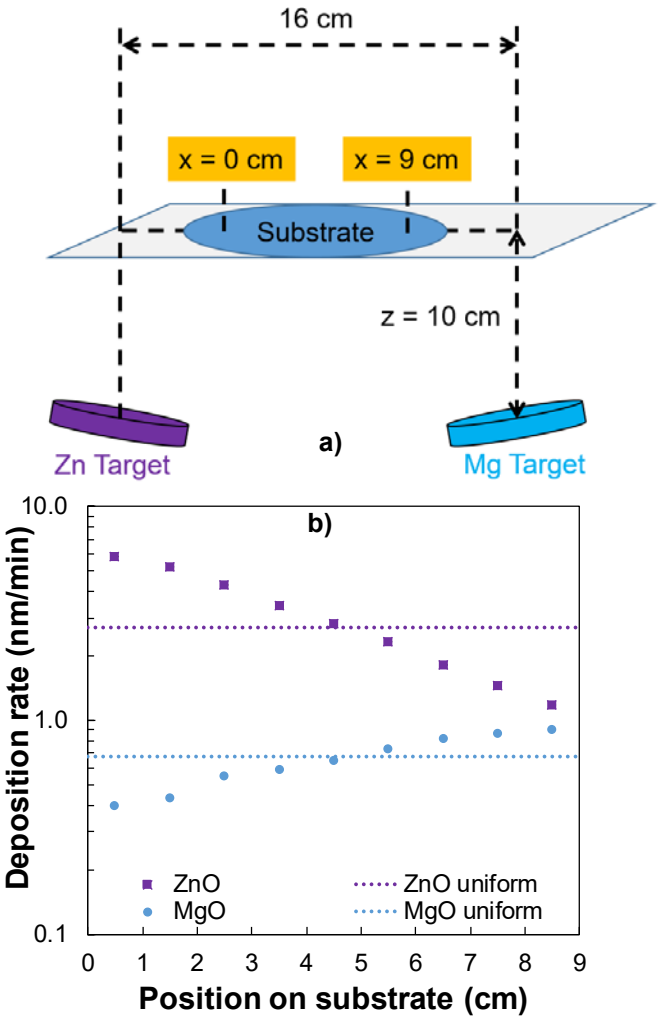

Fig. 1. (a) Two dimensional schematic of the sputter geometry and (b) spatial variation in deposition rate along the line between the two targets for ZnO DC sputtered at 6.9 mA/cm^2 (squares) and MgO RF sputtered at 7.4 W/cm^2 (circles). The horizontal lines indicate the uniform deposition rate obtained under these conditions with sample rotation.

B. Properties of as-deposited MZO

Combinatorial libraries were formed by co-sputtering with the substrate fixed and Figure 2 displays a photograph of a representative library deposited on a silicon wafer, which enabled the smooth and continuous variation to be visualized due to changes in both refractive index and thickness. On glass the libraries are completely transparent by eye. It was found that film composition could be well described by a linear superposition of the deposition rates of the individual targets. The deposition profiles described above enabled combinatorial MZO libraries with more than a 0.4 eV variation in band gap across an 8 cm substrate.

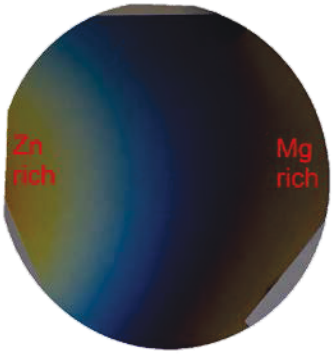

Fig. 2. Picture of a 3-inch Si wafer that visualizes the smooth and continuous variation in both thickness and composition across the combinatorial library.

Figure 3 below shows (a) Tauc plots and (b) the resulting band gap profile along the centerline between the two targets from a library deposited on glass. In this case the band gap varied from 3.4 eV on the Zn-rich side to 4.1 eV on the Mg-rich side, which corresponds to a $Mg_xZn_{1-x}O$ composition gradient ranging from x = 0.05 to x =0.4, respectively [11]. This window spans the range that is expected to be optimal for CdTe solar cells.

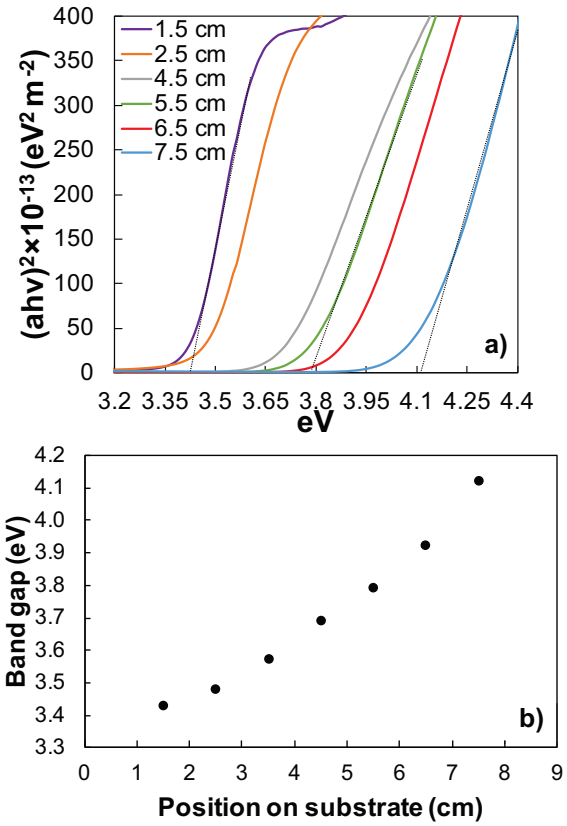

Fig. 3. (a) Tauc plots and (b) the resulting MZO band gap variation along the centerline between the Zn and Mg targets.

Across the range examined all alloys were polycrystalline with a preferential orientation in the (002) direction. Figure 4 shows X-ray diffraction patterns of (002) peak positions for MZO across the substrate. The as-deposited films are crystalline and the peak shift shown in the figure is consistent with an increase in the Mg content. As-deposited films exhibit the ZnO hexagonal structure. It can be seen from the figure that even with some Mg content in the film, the peak is initially shifted slightly in the opposite direction of pure ZnO (002) position. This could indicate presence of stress inside the as-deposited film. Mg content estimated from the band gap was comparable to the expected values based on the deposition rates from each target. However, Vegard's Law consistently underestimated the volume fraction of MgO, which is consistent with a possibility of aforementioned stress in the film.

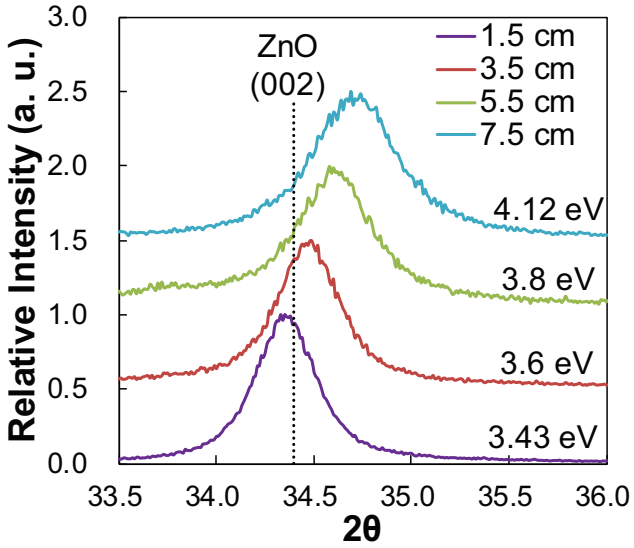

Fig. 4. XRD patterns of (002) peaks of MZO at different positions across the substrate.

Figure 5 below illustrates the change in the work function of MZO film across the substrate as measured by Kelvin probe. Corresponding band gap is plotted on the secondary axis. It can be seen that the work function decreases with increasing Mg content, and therefore increasing band gap. This suggest that the conduction band is shifting upward, which is consistent with theoretical predictions [12]. The change in the work function is ~200 mV greater than the change in the band gap, suggesting that position of either the valence band and/or the Fermi level also increase with increasing Mg content. More data is currently being collected to confirm work function variation.

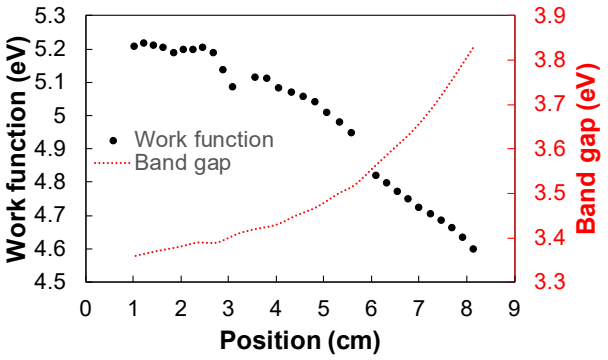

Fig. 5. Variation of work function of MZO film across a substrate with a corresponding band gap plotted on secondary axis.

C. Device performance

To demonstrate the approach preliminary devices were fabricated using a fabrication procedure optimized for CdS-based devices. Using small area devices (0.079 cm^2) it was possible to fit more than 15 columns of devices across a 3-inch substrate. An example of J-V parameters for each column are plotted in Figure 6. It can be seen from the figure that the device performance is correlated with the position on the substrate which in turn corresponds to a difference in Mg content in MZO film across the substrate. Here we see that the maximum efficiency is obtained in devices with maximum FF. V_{oc} is maximized at slightly higher band gap of MZO, which is consistent with what other groups have seen [4, 7].

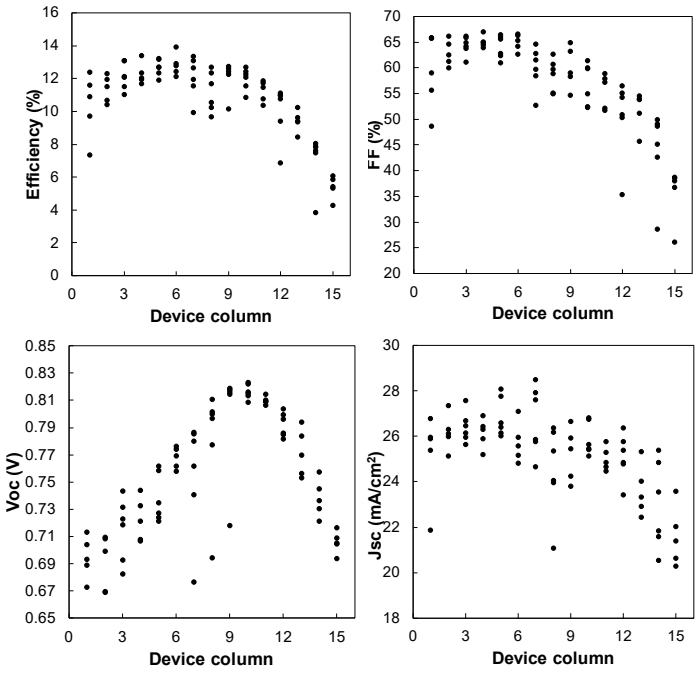

Fig. 6. J-V parameters of devices in each column across a 3-inch substrate

Representative J-V parameters of devices with optimal, too low, and too high band gaps are plotted in Figure 7. When the band gap is too high, electron affinity of the MZO decreases, causing a large barrier at the CdTe interface. This will result in loss of FF and J_{sc} as seen in the figure and is consistent with literature [7]. On the contrary, when the band gap is too low and electron affinity of MZO increases, a so-called "cliff" is formed, causing recombination at the front interface and leading to loss of V_{oc} [7]. The initial performance is promising, especially when considering that the device efficiency is at 14.5% with oxygen present both during CdTe deposition and $CdCl_2$ treatment. Ablekim et. al. [5] saw efficiencies around 10% when oxygen was present during processing. Work is currently to re-optimize various process steps such as $CdCl_2$ activation and our back contact process to improve both FF and V_{oc} at the optimal MZO band gap.

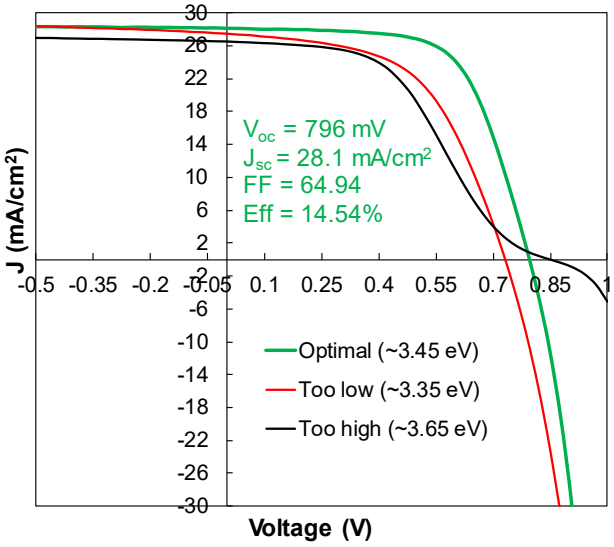

Fig. 7. J-V parameters at optimal, too high, and too low band gaps of MZO.

IV. Summary And Conclusions

In this paper we demonstrate that high quality MZO films can be synthesized by reactive co-sputtering. Combinatorial libraries were formed with smooth and continuous variations in thickness, band gap, and work function. This combinatorial technique offers a quick approach to screen multiple compositions of MZO to optimize performance of CdTe-based solar cells on a single substrate. A band gap of ~3.5 eV was found to be optimal for the current processing conditions in our lab.

Acknowledgments

We are grateful to the National Science Foundation through award number CBET-1706149. This work was authored in part by the Alliance for Sustainable Energy, LLC, the manager and

operator of the National Renewable Energy Laboratory for the U.S. Department of Energy (DOE) under Contract No. DE-AC36-08GO28308. Funding provided by U.S. Department of Energy Office of Energy Efficiency and Renewable Energy Solar Energy Technologies Office. The views expressed in the article do not necessarily represent the views of the DOE or the U.S. Government. The U.S. Government retains and the publisher, by accepting the article for publication, acknowledges that the U.S. Government retains a nonexclusive, paid-up, irrevocable, worldwide license to publish or reproduce the published form of this work, or allow others to do so, for U.S. Government purposes. We would also like to thank Dr. Tursun Ablekim for helpful discussions.

REFERENCES

[1] "Best Research-Cell Efficiencies," *NREL,* 2019. Online at: https://www.nrel.gov/pv/assets/pdfs/pv-efficiency-chart.20190103.pdf

[2] A. H. Munshi, J. Kephart, A. Abbas, J. Raguse, J. N. Beaudry, K. Barth, et al., "Polycrystalline CdSeTe/CdTe Absorber Cells With 28 mA/cm^2 Short-Circuit Current," *IEEE Journal of Photovoltaics*, vol. 8, pp. 310-314, 2018.

[3] A. Kanevce, M. O. Reese, T. M. Barnes, S. A. Jensen, W. K. Metzger, "The roles of carrier concentration and interface, bulk, and grain-boundary recombination for 25% efficient CdTe solar cells," *Journal of Applied Physics,* vol. 121, p. 214506, 2017.

[4] J. M. Kephart, J. W. McCamy, Z. Ma, A. Ganjoo, F. M. Alamgir, and W. S. Sampath, "Band alignment of front contact layers for high-efficiency CdTe solar cells," *Solar Energy Materials and Solar Cells*, vol. 157, pp. 266-275, 2016.

[5] Tursun Ablekim, Craig Perkins, Xin Zheng, Carey Reich, Drew Swanson, Eric Colegrove, Joel N. Duenow, et. al., "Tailoring MgZnO/Cd(Se)Te Interfaces for Photovoltaics," *IEEE Journal of Photovoltaics,* 2018.

[6] J. M. Kephart, A. Kindvall, D. Williams, D. Kuciauskas, P. Dippo, A. Munshi, et al., "SputterDeposited Oxides for Interface Passivation of CdTe Photovoltaics," *IEEE Journal of Photovoltaics*, vol. 8, pp. 587-593, 2018.

[7] T. Song, A. Kanevce, and J. R. Sites, "Emitter/absorber interface of CdTe solar cells," *Journal of Applied Physics*, vol. 119, p. 233104, 2016.

[8] Shengqiang Ren, Huiqin Wang, Yifan Li, Hongyu Li, Rui He, Lili Wu, Wei Li, Jingquan Zhang, Wenwu Wang, Lianghuan Feng, "Rapid thermal annealing on ZnMgO window layer for improvedperformance of CdTe solar cells", *Solar Energy Materials and Solar Cells*, vol. 187, pp. 97-103, 2018.

[9] Francesco Bittau, Christos Potamialis, Mustafa Togay, Ali Abbas, Patrick J.M. Isherwood,Jake W. Bowers, John M. Walls, "Analysis and optimisation of the glass/TCO/MZO stack for thinfilm CdTesolar cells", *Solar Energy Materials and Solar Cells*, vol. 187, pp. 15-22, 2018.

[10] Pravakar P. Rajbhandaria, André Bikowskia, John D. Perkinsa, Tara P. Dhakalb, and Andriy Zakutayev, "Combinatorial sputtering of Ga-doped (Zn,Mg)O for contact applications in solar cells", *Solar Energy Materials and Solar Cells*, vol. 159, pp. 219-226, 2017.

[11] Takashi Minemoto, Takayuki Negami, Shiro Nishiwaki, Hideyuki Takakura, Yoshihiro Hamakawa, "Preparation of $Zn_{1-x}Mg_xO$ films by radio frequency magnetron sputtering", *Thin Solid Films,* vol. 372, pp. 173-176, 2000.

[12] G. Venkata Rao, F. Säuberlich, and A. Klein, "Influence of Mg content on the band alignment at CdS/(Zn,Mg)O interfaces", *Applied Physics Letters,* vol. 87, p. 032101, 2005